



Brown, P., Mohamed, A., Ardyani, T., Rogers, S. E., & Eastoe, J. (2017). Magnetic and Phase Behavior of Magnetic Water-in-Oil Microemulsions. *Journal of Surfactants and Detergents*, 20(4), 799-804.  
<https://doi.org/10.1007/s11743-017-1961-9>

Peer reviewed version

Link to published version (if available):  
[10.1007/s11743-017-1961-9](https://doi.org/10.1007/s11743-017-1961-9)

[Link to publication record in Explore Bristol Research](#)  
PDF-document

This is the author accepted manuscript (AAM). The final published version (version of record) is available online via WILEY at <http://onlinelibrary.wiley.com/doi/10.1007/s11743-017-1961-9/abstract;jsessionid=DF277F8BA777E838163B64457B36C4F0.f02t01> . Please refer to any applicable terms of use of the publisher.

## University of Bristol - Explore Bristol Research

### General rights

This document is made available in accordance with publisher policies. Please cite only the published version using the reference above. Full terms of use are available:  
<http://www.bristol.ac.uk/pure/about/ebr-terms>

# Magnetic and Phase Behaviour of Magnetic water-in-oil Microemulsions

Paul Brown<sup>a</sup>, Azmi Mohamed<sup>b\*</sup>, Tretya Ardyani<sup>b</sup>, Julian Eastoe<sup>c</sup>,

<sup>a</sup>*Department of Chemical Engineering, Massachusetts Institute of Technology, Cambridge, MA, 02139, USA;* <sup>b</sup>*Department of Chemistry, Faculty of Science and Mathematics, Universiti Pendidikan Sultan Idris, 35900 Tanjong Malim, Perak, Malaysia;* <sup>c</sup>*School of Chemistry, University of Bristol, Bristol BS8 1TS, UK.*

\*Correspondence: azmi.mohamed@fsmt.upsi.edu.my

## Abstract

Magnetic water-in-oil microemulsions with anisotropic morphology have been generated by mixing single-chain magnetic surfactants (dodecyltrimethylammonium trichloromonobromoferrate, DTAF) with non-magnetic di-chain analogues (didodecyldimethylammonium bromide, DDAB). Full phase diagrams have been mapped as a function of surfactant composition, water content, and temperature. It was shown that for all surfactant concentrations  $[\text{Surfactant}_{\text{total}}]$ , on replacing 30wt% DDAB with DTAF optimum  $w$  ratios could be achieved; up to  $w = 120$  for  $[\text{Surfactant}_{\text{total}}] = 0.050\text{M}$ . Small-angle neutron scattering (SANS) indicated that microemulsions droplets had a rod-like morphology with a radius commensurate with the surfactant tail length and an aspect ratio between 6 and 35. In the presence of a large magnetic field (6.7 T) no reorientation of the droplets was observed by SANS.

## Introduction

Magnetic surfactants are a relatively new class of stimuli responsive surfactants [1]. Their magnetic properties derive from metal ions either chelated to a surfactant headgroup [2] or existing as a counterion [3]. Over the past 5 years magnetic surfactants have found demonstrated application ranging from protein separations [4] and DNA manipulation [5], to water remediation [6] and soft colloidal templates [7]. Nanoparticle-free magnetic emulsions have also been generated using magnetic surfactants offering an alternative to Pickering-emulsions [8], which require pre-synthesized nanoparticles limiting scale up applications. Like emulsions, microemulsions have widespread industrial application [9] and also offer much

[Type text]

promise as drug delivery systems [10]. They may be considered as being related to emulsions [11] (i.e. droplet type dispersions either of oil in water (o/w) or of water-in-oil, with a size range in the order of 1 – 50 nm in drop radius). However, unlike emulsions, once the conditions are right, microemulsions form spontaneously and are thermodynamically stable mixtures. Magnetically-responsive microemulsions generated from lanthanide based magnetic surfactants have been reported but detailed structural investigation were not undertaken [12] and magnetic experiments were limited to SQUID magnetometry and did not look at changes in microemulsion structure. The only other study of magnetic microemulsions using magnetic surfactants was not conclusive. The authors used small-angle neutron scattering to ascertain if such structural control was possible. Under an applied 1.6 T field almost no variation between scattering profiles was detected, though the difference was measurable [13].

In this paper, we report mixed surfactant microemulsions generated by blending a traditional di-chain surfactant di-*n*-didodecyldimethylammonium bromide, DDAB, with a single chain magnetic analogue dodecyltrimethylimidazolium trichloromonobromoferrate, DTAF. Such surfactant mixtures are often employed in a wide variety of applications as they give rise to enhanced performance over individual components [14]. In most cases, surfactant synergism is the only way to reach the low surface tensions required (approximately  $0.01 \text{ mN m}^{-1}$ ) for microemulsion formation. The phase behaviour and stability of the mixed surfactant magnetic microemulsions has been characterized and droplet movement in a magnetic field has been investigated using small-angle neutron scattering (SANS). The study demonstrates how magnetic surfactants can replace conventional surfactants in formulations and may help those interested in designing novel tunable nanomagnets [12] and spin-glass systems [15]. Finally, using SANS in a strong magnetic field, it was clear that manipulation of the droplets was not possible. This is perhaps a surprising result considering each droplet contains more magnetic material than other magnetic colloidal systems reported in literature [4], which can be manipulated on the nanoscale. This result may have important implications in development of performance surfactants for applications such as enhanced oil recovery and treatments fluids. For example, bulk microemulsions that respond to a magnetic field may be useful for enhanced oil recovery [16, 17] or as viscosified treatment fluids [18]. In particular the use of magnetic treatment fluids comprising magnetic surfactants has recently been patented [19]. However, if the individual droplets do not orientate themselves in the magnetic field then enhanced magneto-rheological effects may be limited. It is anticipated that this study

will prompt further research into the origins of magnetism in surfactant based systems and help determine potential applications.

## **Experimental**

### **Materials and Synthesis**

Dodecyltrimethylammonium bromide (DTAB, 99%) iron trichloride (99.9%), didodecyltrimethylammonium bromide (99%, DDAB) and *n*-heptane (<99) were bought from Sigma Aldrich. *n*-Heptane, is known to contain surface-active impurities. Prior to making microemulsions, heptane was purified by washing with fuming sulfuric acid, then neutralising with 10 wt% sodium bicarbonate (aq.) with chemical purity being assessed by interfacial tension measurements [20].

Dodecyltrimethylammonium trichloromonobromoferrate (DTAF) was synthesized according to literature [3]. In brief 1eq. dodecyltrimethylammonium bromide (Sigma, 99%) was mixed with iron trichloride (Sigma, 99.9%) in methanol for 1 hour. The solvent was then removed under reduced pressure and the surfactant dried *in vacuo* for 48 hours. Purity was characterized by elemental analysis and UV-Vis spectroscopy [3]. Experimental and theoretical (brackets) as % wt. DTAF: C 38.29 (38.31), H 7.22 (7.23), N 2.98 (2.97).

### **Interfacial Tension Measurement at water/*n*-heptane interface**

The interfacial tension (IFT) at a water/*n*-heptane interface in the presence of a surfactant was measured with the pendant-drop tensiometer developed in our laboratory. The following procedure was carried out for the measurements. For the measurement Water/*n*-heptane microemulsions containing DTAF/DDAB mixtures at the total surfactant concentration of 0.1M were prepared at the constant water-to-surfactant molar ratio of 10 and DDAB concentrations of 100, 90, 80, 70, and 60 wt% in total surfactant mass. A glass syringe with the needle gauge 28 (o.d. 0.362 mm and i.d. 0.184 mm) was used to form pendant droplets in the microemulsions contained in a quartz cell. When a water droplet was formed at the tip of the needle in the microemulsions, water began to dissolve in the microemulsion and the size of the drop reduced. Thus, by adding water from the syringe, the size of the droplet was kept almost constant. Once a suitable droplet was formed, a photograph of the droplet was taken and used for calculation of IFT value.

The IFT was determined from the shape of the droplet using axisymmetric drop shape analysis (ADSA) based on the Laplace equation. [21-24] In the analysis, the densities of the *n*-heptane-rich and water-rich

phases were assumed to be equal to those of their respective pure constituents. Several images of the droplet were taken at certain time intervals to attain thermodynamic equilibrium, until the variation in the observed IFT became smaller than 0.1 mN/m per 20 min. At least 5 drops were formed under each experimental condition to obtain an average value.

### Microemulsion Formation

Microemulsions were prepared by weighing the required amounts of DDAB and DTAF (weighed using a four-figure balance with an accuracy of  $\pm 0.1$  mg) into clean, 5 ml volumetric flasks, then required volumes of water were added (using a Hamilton microsyringe). Next, a few microlitres of heptane was added and the mixture vortexed until all the surfactant dissolved. Finally, more heptane was added up to the 5 mL mark and samples were shaken thoroughly to attain equilibrium. Samples were then left for 48 hours (owing to phase resolution) and characterized by visual inspection. For subsequent concentration studies, serial dilution was used.

### Small-Angle Neutron Scattering

Experiments were carried out using the SANS2d instrument at the Rutherford Appleton Laboratory, ISIS, U.K. An incident wavelength range of 2.2–14 Å, with the 1m<sup>2</sup> detector offset sideways and vertically by 150 mm, was used resulting in an effective  $Q$  range of 0.005–0.7 Å<sup>-1</sup> was used. The measurements gave the absolute scattering cross section  $I(Q)$  (cm<sup>-1</sup>) as a function of momentum transfer  $Q$  (Å<sup>-1</sup>). Absolute intensities ( $\pm 5\%$ ) were determined by calibrating the received signal from a partially deuterated polymer standard, which was corrected for sample transmission and cell and solvent backgrounds, as reported previously.

The neutron scattering intensity as a function of scattering vector,  $I(Q)$ , is dependent on the number density of scattering bodies,  $N_p$ ; the difference in scattering length density between the scattering body and the solvent ( $\Delta\rho$ ); the particle volume,  $V_p$ ; the form factor,  $P(Q)$ , which describes particle size and shape; and the background incoherent scattering [25], and is described as follows

$$I(Q) = N_p V_p^2 (\Delta\rho)^2 P(Q) S(Q) + B_{inc} \quad (1)$$

A model for rods was used to fit the data in SASView, which describes both  $P(Q)$  and  $S(Q)$  [26]. The form factor for randomly oriented rods in solution is given by equation 2 and 3, yielding rod length and cross-sectional radius,  $R$ .

$$P(Q, \alpha) = \frac{scale}{V} f^2(Q) + bkg \quad (2)$$

$$f(Q) = 2(\Delta\rho) \frac{\sin\left(\frac{1}{2QL\cos\alpha}\right)}{\frac{1}{2QL\cos\alpha}} \frac{J_1(Qrsin\alpha)}{Qrsin\alpha} \quad (3)$$

where the scale is proportional to the volume fraction of the rods,  $V$  is the volume of the rod,  $L$  is the length,  $r$  the radius,  $J_1(x)$  the first order Bessel function of the first kind,  $\alpha$  is the angle between the axis of the rod and the  $Q$ -vector, and  $\Delta\rho$ , the contrast (difference between scattering length density of particle and solvent:  $\rho_{H_2O} = -0.56 \times 10^{10} \text{ cm}^{-2}$ ,  $\rho_{n\text{-heptane (d16)}} = 6.30 \times 10^{10} \text{ cm}^{-2}$ ).

Magnetic fields were applied using a 7.5 T cryomagnet, with the beam passing through ‘narrow’ windows and across the diameter of the coils. Further details may be found on the STFC ISIS website.

## Results and discussion

### Interfacial Tension

A prerequisite to microemulsion formation is an ultra-low interfacial tension between the oil and water phases,  $\gamma_{o/w}$ . A surfactant is used to reduce  $\gamma_{o/w}$  sufficiently (lowering energy required to increase surface area) so that spontaneous dispersion of water or oil droplets occurs and the system is thermodynamically stable. The pendant drop technique was used to measure the interfacial tension of the water-heptane interface as a function of surfactant ratio (Table 1). A low interfacial tension of around  $1.79 \text{ mN m}^{-1}$  was recorded for pure DDAB. This decreased upon addition of the single chain DTAF until at relatively small amounts the interfacial tension was too low to measure, demonstrating that these magnetic surfactant blends perform just like conventional surfactants.

**Table 1:** Interfacial tension data for water-in-heptane microemulsions with DDAB and DTAF mixtures

---

Water/n-heptane interfacial tension / ( $\text{mN m}^{-1}$ )

---

Run	DDAB:DTAF	DDAB:DTAF	DDAB:DTAF
	100:0	90:10	80:20
1	1.66	1.63	-
2	1.74	1.47	-
3	1.85	1.63	-
4	1.82	1.50	-
5	1.88	1.44	-
Average	1.79	1.53	-

## Microemulsion Formation

In this work, phase behaviour was investigated as a function of surfactant ratio (in wt %) and  $w$  value ( $w = [\text{water}] / [\text{surfactant}]$ ) at various surfactant concentrations (Figure 1) and also as a function of temperature at constant surfactant concentration (Figure 2) in order to locate phase boundaries. Single-phase ( $1\Phi$ ) w/o microemulsions were identified (by visual inspection). Samples with faint turbidity or small water droplets settling out, were taken to be at the emulsification boundary ( $w_{\max}$ ).

D<sub>2</sub>O-DDAB-*n*-heptane microemulsion systems have been studied before, exhibiting two distinct phase separations regions (WII and  $1\Phi$ ) [27]. By partially replacing DDAB with the single chain DTAB, Eastoe *et al.* showed that the single-phase region shifted to higher  $w$ , meaning that higher DTAB content both increased maximum water solubilization ( $w_{\max}$ ) and the amount of water required to stabilize the microemulsions ( $w_{\min}$ ). They demonstrated that microemulsion phase behaviour was affected by surfactant bulk composition and changes in the effective packing parameter as a result of surfactant mixing at the D<sub>2</sub>O-heptane interface. The single-chained DTAB prefers to be curved toward the oil (positive curvature,  $v/a_h l_c \sim 0.65$ ), whereas the double-chained surfactant curves towards water (negative curvature,  $v/a_h l_c \sim 1.30$ ). Here curvature depends on both surfactant type but also on the oil-water interface. Replacing DDAB by DTAB decreases the average chain volume, whilst the area per surfactant head group remains almost constant. Hence the mean packing parameter of the surfactant mixture decreases.

Instead of using DTAB, our studies used the structurally analogues but magnetically-responsive surfactant DTAF. It is important to note that conductivity data and SANS show only small changes in physico-chemical properties of these surfactants on changing the anion from Br<sup>-</sup> to FeCl<sub>3</sub>Br<sup>-</sup> [3].

The phase behaviour of DDAB-DTAF systems (Figure 1) compares with the studies for DDAB-DTAB systems, and is almost independent of overall surfactant content [28]. Increasing DTAF content to around 30 wt% leads to  $w_{\max} = 120$  (for 0.050 M surfactant system) for a single-phase. This is consistent with the

interfacial tension analysis. Above the solubilization boundary, the w/o microemulsion is present in co-existence with an excess water phase (i.e. Winsor II (WII) system).

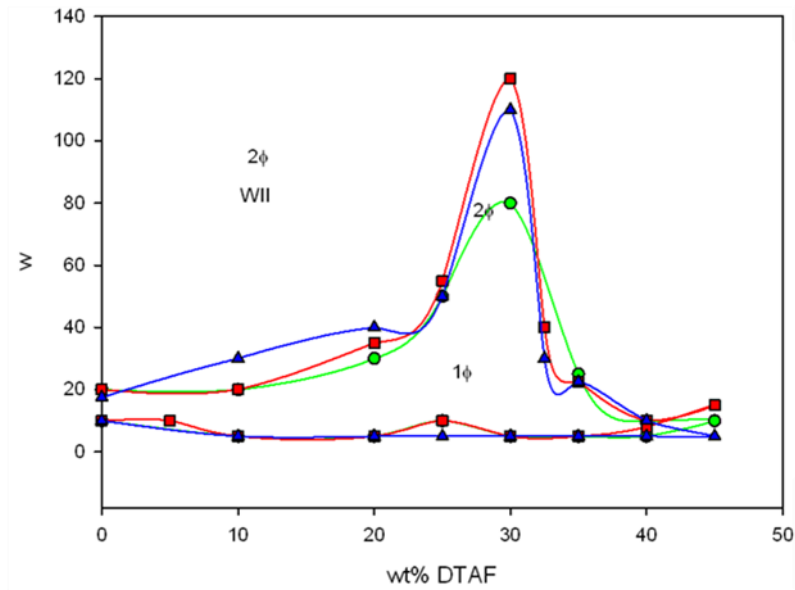


**Figure 1:** Phase diagram as a function of surfactant ratio (DDAB:DTAF) ,  $w$  value and total surfactant concentration at 25 °C. [Surfactant<sub>total</sub>]: 0.100 M (green circle), 0.050 M (red square), 0.025 M (blue triangle). 1 $\phi$  represents a single isotropic phase; and 2 $\phi$ / WII represents a two phase system whereby the upperlayer is a microemulsion and the lower layer contains excess water.

There are two effects of temperature for ionic surfactant systems: (i) an increase in the electrostatic repulsions between the surfactant headgroups (due to higher counter-ion dissociation), causes a decrease in film curvature; (ii) more gauche conformations are induced in the surfactant chains, which become more coiled, resulting in an decrease in curvature [29, 30]. It is understood that the combined effects are competitive with the electrostatic term believed to be slightly dominant, so curvature increases weakly with increasing temperature [27]. [PB1]The results in this paper appear broadly agree with this (Figure 2). For 0.10 M total surfactant concentration on increasing the temperature from -18 °C up to 25 °C the single phase region increases. However, on increasing the temperature further to 55 °C a dramatic decrease in the single phase region occurs. This is probably owing to a change in dominance whereby tail group conformation becomes more important.



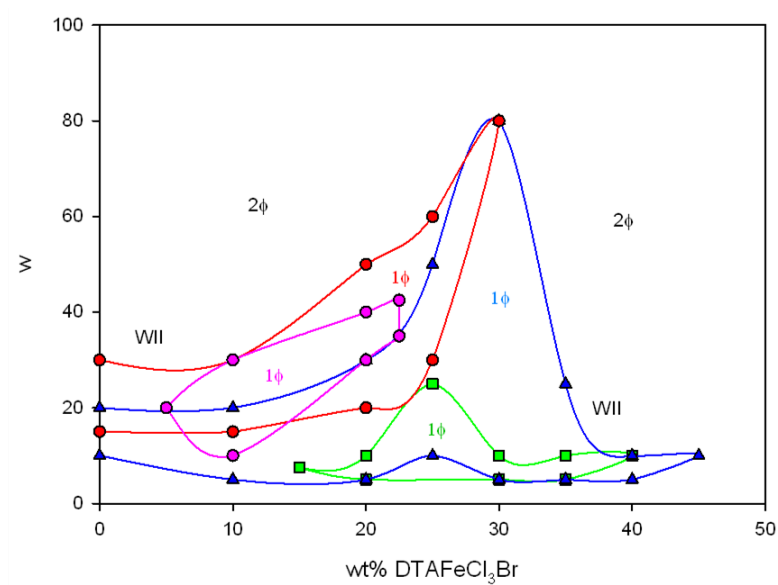


**Figure 2:** Phase diagram at constant surfactant concentration (0.10 M), as a function of surfactant ratio (DDAB:DTAF),  $w$  value and temperature. Temperature: 55 °C (green square), 25 °C (blue triangle), 5 °C (red circle), -18 °C (pink circle). 1 $\phi$  represents a single isotropic phase; and 2 $\phi$ / WII represents a two phase system whereby the upperlayer is a microemulsion and the lower layer contains excess water.

### Small-Angle Neutron Scattering

Small-angle neutron scattering (SANS) conclusively shows the structure of the microemulsions as a function of surfactant ratio at constant  $w$  value and overall surfactant concentration. The profiles are consistent with non-interacting rods (Figure 3, Table 2) whereby increasing the DTAF (single chain) content leads to a reduction in rod length. At high  $q$  the scaling of  $Q^{-4}$  indicates a sharp, smooth water/oil interface.

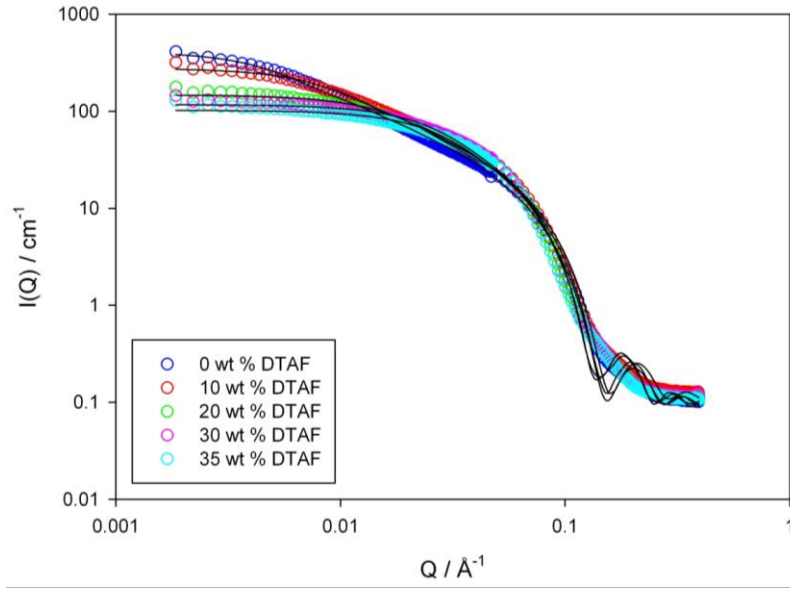


**Figure 3:** SANS profiles for H<sub>2</sub>O-in-*d*-heptane mixed micelles using DDAB-DTAF at a fixed total surfactant concentration of 0.100 M surfactant at 25 °C. Lines are fits using a model for rods.

**Table 2:** Parameters fitted to SANS data using the model for rods.

wt % DTAF	$w$	Type	Shape	$R / \text{\AA}$	$L / \text{\AA}$
0	10	1 $\Phi$	rod	25	874
10	10	1 $\Phi$	rod	25	495
20	10	1 $\Phi$	rod	26	252
30	10	1 $\Phi$	rod	28	170
35	10	1 $\Phi$	rod	28	159

SANS experiments were repeated in the presence of a 6.7 T magnetic field. However, the anisotropic microemulsions appeared not to orientate themselves even in very large fields (6.7 T) as indicated by the SANS profiles, which remained consistent with those pre-field (data not shown as exact overlay observed). This was an unexpected result but may potentially be that only orientation of spin occurs which does not lead to the movement of the microemulsion; unlike other colloidal systems [31, 32]. At first glance, one might assume it is simply due to small particle size and low concentrations of magnetic material. However, in the case of myoglobin (Mb, 11.6  $\mu\text{M}$ ,  $M_w \sim 17$  kDa) surrounded by a corona of magnetic surfactant ( $\sim 3.0$  mM) the conjugates may be concentrated in a weak (0.2T) magnetic field [33]. In this system it may be estimated that there are around 261 surfactant molecules per protein spread over a volume of around 22 nm<sup>3</sup> (assuming Mb diameter = 3.5 nm and is spherical [34]), whereas in the microemulsion studied in this paper ( $w=10$ , 35wt% DTAF) there are  $\sim 600$  molecules of surfactant per droplet (droplet volume  $\sim 522$  nm<sup>3</sup>, assuming a

capped cylinder calculated from SANS and no free surfactant molecules in solution). One reason may be the time scale of the experiments but this requires further investigation.

In conclusion, this paper demonstrates how magnetic microemulsions can be formed from a combination of surfactants, which allows for easy control of microemulsion size and shape. This should be useful for the future study of nanomagnet design [15]. We demonstrate that although bulk microemulsions can be manipulated in a magnetic field [12] individual droplets could not according to SANS. This has ramifications when developing magnetic surfactants for specific applications such as treatment fluids for oilfields.

## Acknowledgments

Fundamental Research Grant Scheme (FRGS; Grant code: 2015-0155-101-02) and Kurita Water and Environment Foundation (KWEF; Grant code: 2016-0142-102-11)

## References

1. P. Brown, C. Butts, J. Eastoe, Stimuli-Responsive Surfactants, *Soft Matter*, **2013**, 9, 2365-2374.
2. S. Polarz, C. Bährle, S. Landsmann, A. Kläiber, Panoramic Structures by Hierarchical Cascade Self-Assembly of Inorganic Surfactants with Magnetic Heads Containing Dysprosium Ions, *Angew. Chem. Int. Ed.*, **2013**, 52, 13665-13670.
3. P. Brown, A. Bushmelev, C. P. Butts, J. Cheng, J. Eastoe, I. Grillo, R. K. Heenan, A. M. Schmidt, Magnetic Control over Liquid Surface Properties with Responsive Surfactants, *Angew. Chem. Int. Ed.*, **2012**, 51, 2414-2416.
4. P. Brown, L. Bromberg, M. I. Rial-Hermida, M. Wasbrough, T. A. Hatton, C. Alvarez-Lorenzo, Magnetic Surfactants and Polymers with Gadolinium Counterions for Protein Separations, *Langmuir*, **2016**, 32, 699-705.
5. L. Xu, L. Feng, J. Hao, S. Dong, Controlling the Capture and Release of DNA with a Dual-Responsive Cationic Surfactant, *ACS Appl. Mater. Interfaces*, **2015**, 7, 8876-8885.
6. T. M. McCoy, P. Brown, J. Eastoe, R. F. Tabor, Noncovalent Magnetic Control and Reversible Recovery of Graphene Oxide Using Iron Oxide and Magnetic Surfactants, *ACS Appl. Mater. Interfaces*, **2015**, 7, 2124-2133.
7. S. Kim, C. Bellouard, A. Pasc, E. Lamouroux, J. L. Blin, C. Carteret, Y. Fort, M. Emo, P. Durand, M. J. Stébé, *J. Mater. Chem.*, **2013**, 1, 6930-6934.
8. A. Kaiser; T. Liu; W. Richtering; A. M. Schmidt, Magnetic Capsules and Pickering Emulsions Stabilized by Core-Shell Particles, *Langmuir*, **2009**, 25, 7335.

9. J. Klier, C. J. Tucker, T. H. Kalantar, D. P. Green, Properties and Applications of Microemulsions, *Adv. Mater.*, **2000**, 12, 1751-1757.
10. S. Talegaonkar, A. Azeem, F. J. Ahmad, R. K. Khar, S. A. Pathan, Z. I. Khan, Microemulsions: a novel approach to enhanced drug delivery, *Recent Pat. Drug Deliv. Formul.*, **2008**, 2, 238-257.
11. *Microemulsions. Background, New Concepts, Applications, Perspectives*. Ed. Cosima Stubenrauch, John Wiley & Sons, Hoboken, **2008**.
12. P. Brown, C. P. Butts, J. Eastoe, S. Glatzel, I. Grillo, S. H. Hall, S. Rogers, K. Trickett, Microemulsions as tunable nanomagnets, *Soft Matter*, **2012**, 8, 11609-11612.
13. P. Brown, T. A. Hatton, J. Eastoe, Magnetic Surfactants, *Curr. Opin. Coll. Int. Sci.*, **2015**, 20, 140-150.
14. A. Bera, K. Ojiha, A. Mandal, Synergistic Effect of Mixed Surfactant Systems on Foam Behavior and Surface Tension, *J. Surf. Deterg.*, **2013**, 16, 621-630.
15. P. Brown, G. N. Smith, E. P. Hernandez, C. James, J. Eastoe, W. C. Nunes, C. M. Settens, T. A. Hatton, P. J. Baker, Magnetic surfactants as molecular based magnets with spin glass-like properties, *J. Phys. Condens. Matter*, **2016**, 28, 176002.
16. A. Bera, A. Mandal, Microemulsions: a novel approach to enhanced oil recovery: a review, *J. Pet. Explor. Prod. Technol.*, **2015**, 5, 255-269.
17. N. Pal, K. Babu, A. Mandal, surface tension, dynamic light scattering and rheological studies of a new polymeric surfactant for application in enhanced oil recovery, *J. Petrol Sci. Eng.*, **2016**, 146, 591-600.
18. A. Loiseau, Y. Chen, Pickering emulsion treatment fluid, US 9388335 B2, **2016**.
19. R. J. Murphy, Treatment fluids comprising magnetic surfactants and methods relating thereto, US 9284476 B2, **2016**.
20. W. L. F. Armarego, C. L. L. Chai, *Purification of Laboratory Chemicals*, Butterworth-Heinemann, **2013**.
21. J. W. Jennings, N. R. Pallas, An efficient method for the determination of interfacial tensions from drop profiles, *Langmuir*, **1988**, 4, 959-967.
22. Y. Rotenberg, L. Boruvka, A. W. Neumann, Determination of surface tension and contact angle from the shapes of axisymmetric fluid interfaces, *J. Colloid Interface Sci.*, **1983**, 93, 169-183.
23. D. Li, P. Cheng, A. W. Neumann, Contact angle measurement by axisymmetric drop shape analysis (ADSA), *Adv. Colloid Interface Sci.*, **1992**, 39, 347-382.
24. O. I. del Río, A. W. Neumann, Axisymmetric Drop Shape Analysis: Computational Methods for the Measurement of Interfacial Properties from the Shape and Dimensions of Pendant and Sessile Drops, *J. Colloid Interface Sci.*, **1997**, 196, 136-147.
25. King, S. M. *Small-angle neutron scattering. In Modern Techniques for Polymer Characterization*; Pethrick, R. A.; Dawkins, J. V., Eds.; John Wiley: New York, **1999**.
26. Rice, S. A. *Small Angle Scattering of X-rays*; Guinier, A.; Fournet, G., Eds.; Wiley: New York, 1955; 268 pp; *J. Polym. Sci.* **1956**, 19, 594– 594.

27. A. Bumajdad; J. Eastoe, Conductivity of water-in-oil microemulsions stabilized by mixed surfactants, *J. Coll. Int. Sci.*, **2004**, 274, 268-276.
28. T. Cosgrove, *Colloid Science Principles, Methods and Applications*. 2nd Ed.; Wiley: London, **2010**.
29. L. Magnus Bergström; V. M. Garamus, Structural behaviour of mixed cationic surfactant micelles: A small-angle neutron scattering study, *J. Coll. Int. Sci.*, **2012**, 381, 89-99.
30. A. Y. E. A. Bumajdad. Phase structure and interfacial composition of mixed surfactant microemulsions. University of Bristol, Bristol, **2000**.
31. A. Kawamura, M. Kohri, T. Taniguchi, K. Kishikawa, Surface Modification of Polydopamine Particles via Magnetically-Responsive Surfactants, *Trans. Mat. Res. Soc. Japan*, **2016**, 41, 301-304.
32. P. Beck, M. Liebi, J. Kohlbrecher, T. Ishikawa, H. Ruegger, H. Zepik, P. fischer, P. Walde, E. Windhab, Magnetic field alignable domains in phospholipid vesicle membranes containing lanthanides, *J. Phys. Chem. B*, **2010**, 114, 174-186.
33. P. Brown, A. M. Khan, J. P. Armstrong, A. W. Perriman, C. P. Butts, J. Eastoe, Magnetizing DNA and proteins using responsive surfactants, *Adv. Mater.*, **2012**, 24, 6244-6247.
34. S. Papadopoulos, K. D. Jürgens, G. Gros, Protein diffusion in living skeletal muscle fibers: dependence on protein size, fiber type, and contraction, *Biophys. J.* **2000**, 79, 2084-2094.